Simultaneous Optimal Parameter and Mode Transition Time Estimation

Lauren M. Miller and Todd D. Murphey[1]

***Abstract*— This paper presents a method of simultaneous mode transition time and parameter estimation for hybrid systems based on switching time optimization techniques. A concise derivation of first- and second-order optimality conditions with respect to both mode transition times and parameter values is presented, including cross-derivative terms between the switching times and the parameters. The estimation algorithm is shown to be effective for estimating transition times as well as unknown parameter values from coarsely sampled data for a skid-steered vehicle, which traverses unknown or changing terrain and transitions between discrete dynamic modes. It is shown that second-order optimization methods using the exact Hessian provide far superior convergence, compared to first- or approximate second-order methods, to correct values in simulated and experimental scenarios.**

I. Introduction

There are many systems in robotics that experience discrete transitions between continuous modes. A method for robustly estimating when transitions occur based on potentially coarse data is necessary due to modeling and parametric uncertainty in real-world systems. Operation in unknown environments presents the additional need for terrain parameter identification. This paper focuses on estimating mode transition time and parameter values using optimization techniques. It will be shown that these two problems are nontrivially coupled.

A method is presented that utilizes second-order optimality conditions for nonlinear time-varying systems to achieve fast convergence. The gradient and the Hessian of an objective function representing a measure of the error from the estimated trajectory to the measured data (e.g. least-squares) are derived, with respect to both mode switching times and parameters. Although similar calculations with respect to switching times [1] and parameters [2] independently have been derived in previous work, the derivations presented here are based on introductory calculus techniques. The proof is extended to hybrid systems, and the techniques generalize to cross-derivative terms which are critical in achieving fast convergence and provide sufficient conditions for optimality.

Simulated and experimental results demonstrate that this method is efficient for estimating the mode transition times and parameter values that generate a trajectory that optimally fits coarse GPS data obtained for a skid-steered vehicle. First- and second-order optimization algorithms were compared in simulation, using both the exact and block-diagonal approximated Hessian. The importance of the cross-derivative terms of the exact Hessian in achieving fast convergence, only possible to define when estimating mode switches and unknown parameters simultaneously, is demonstrated.

[1]The authors are with the Department of Mechanical Engineering, Northwestern University, Evanston, IL, 60208 USA (e-mail: LaurenMiller@U.Northwestern.edu, T-Murphey@Northwestern.Edu

A. Motivating Example: The Skid-Steered Vehicle

Skid-steered vehicles (SSVs) present a challenge from modeling, trajectory-tracking, and control design perspectives. SSVs can turn only by skidding laterally, which introduces dynamics that are distinct from forward rolling and dependent on typically uncertain environmental factors, such as friction. This uncertainty generally necessitates either robust control techniques or accurate models of the vehicle dynamics and environmental parameters, the latter of which will be addressed in this paper.

The SSV in this paper is modeled as a switched system, with modes dependent on whether or not the wheels are slipping with respect to the ground. The vehicle used in experiments is shown in Fig. 1. It is assumed that the number and order of mode transitions are known in advance, a reasonable assumption as mode order is often predictable if the driver inputs to the vehicle are known. Uncertainty in environmental parameters, however, results in variations in the transition times and the vehicle path. It is therefore desirable, given the control inputs, system model, and potentially coarse positional tracking data, to have a method of estimating transition times and parameters in order to represent the continuous path of the vehicle for localization and planning.

B. Related Work

A great deal of research exists on modeling and control of vehicles, as well as mode estimation and online parameter estimation. Localization for vehicles subject to slip often

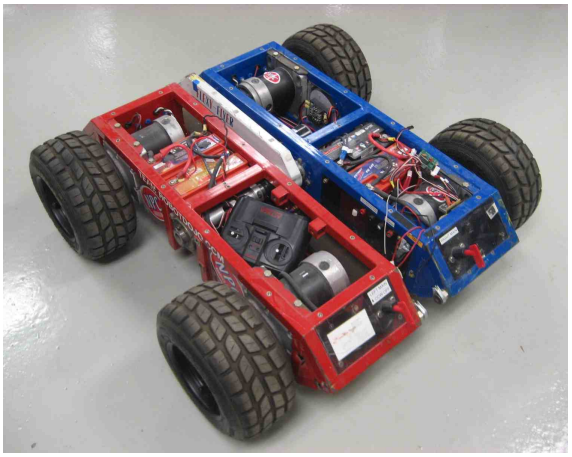

Fig. 1. Skid-Steered vehicle used in experiments

involves complex sensor fusion techniques [3], [4]. Much of the literature regarding vehicle dynamics in general either limits the scope of the analysis or makes assumptions regarding the operating mode or environment ahead of time, allowing for continuous analysis. In many cases, dynamics modes for vehicles, e.g driving, braking, or turning are analyzed independently [5]–[7]. Terrain is also assumed to be known in advance in many cases and to be consistent over the entire trajectory of interest, requiring offline calibration [7]–[13].

There are several mathematical approaches to estimating both switching times and parameters online. Multiple hypothesis testing is one way in which the class of switching time and parameter identification problems has been solved [14], however these approaches are subject to combinatorial complexity. Numerical optimization is presented in [15] for parameter estimation in impulsive systems with unknown parameters. The results we present, however, provide an efficient way of using exact second-order optimization methods. Our approach extends the results derived in [2] to hybrid systems and to the cross-derivative terms.

II. Problem Definition

The goal is to identify, given a set of sampled data, when a switch between modes occurs, as well as the value of a given set of parameters which may differ between modes, or be present in only a subset of them. In the following calculations, it is assumed that the number of switches as well as the mode order are known. Since the control inputs to the vehicle are known, the order and number of transitions from sticking to slipping is predictable.

A general hybrid system with n dimensions, N transitions, and M parameters of interest can be described by a sequence of dynamic equations of the form

$$\dot{x} = f_i(x(t), t) \;\; \tau_i < t < \tau_{i+1} \;, \quad x(t_0) = x_0 \tag{1}$$

for transition times $\tau = \tau_1, \ldots, \tau_N$ and parameters $p = p_1, \ldots, p_M$, where $\tau_0 = t_0$ is the initial time and $\tau_{N+1} = t_f$ is the final time. Note that throughout this paper, $x(t)$ is written when it should explicitly be $x(\tau_1, \ldots, \tau_N, p_1, \ldots, p_M, t)$, and $f(x(t), t)$ should explicitly be $f(x(t), \tau_1, \ldots, \tau_N, p_1, \ldots, p_M, t)$.

Unknown switching times and parameters can be estimated simultaneously by minimizing an objective function of the form

$$J(\tau_1, \ldots, \tau_N, p_1, \ldots, p_M) = \int_{t_0}^{t_f} \ell(x(t), t) dt, \tag{2}$$

where $\ell(x(t), t)$ is an arbitrary incremental cost function, such as $(x(t) - x_{ref}(t))^T (x(t) - x_{ref}(t))$. It is assumed that $\ell(x(t))$ does not depend explicitly on the switching times or parameters.

Although not addressed here, there are scenarios where the order in which mode changes occur is not known. A method for determining mode order is provided in [1]. Additionally, while in this paper the trajectory $x(t)$ is assumed to be a continuous signal, impulsive optimization techniques [15] would allow the extension of this method to non-continuous state variables.

A. Optimization Methods

First- and second-order iterative optimization algorithms are compared. Steepest descent is a first-order algorithm which takes a step at each iteration in the direction of the negative gradient. Steepest descent is a global method and depends only on first-order information, but results in linear convergence which is typically slow and impractical for real-time implementation.

Sequential Quadratic Programming (SQP) is used as a constrained, second-order optimization method, providing drastically reduced convergence time in convex regions [16]. SQP involves solving a quadratic program at each iteration, subject to a set of constraints on the order of the switching times, requiring calculation of both the gradient and the Hessian. The exact Hessian, which involves the cross-derivative terms between the switching times and parameters, i.e.

$$\text{exact Hessian} : \begin{pmatrix} D_\tau^2 J & D_p D_\tau J \\ D_\tau D_p J & D_p^2 J \end{pmatrix} \tag{3}$$

is derived in Section IV. The effects of using an approximate, block-diagonal Hessian, which does not include the cross-derivative terms,

$$\text{block-diagonal Hessian} : \begin{pmatrix} D_\tau^2 J & 0 \\ 0 & D_p^2 J \end{pmatrix} \tag{4}$$

are also examined. Both the SQP and steepest descent algorithms are well-established. For more information, see [16].

For the skid-steered vehicle example in Section V, a combination of steepest descent and SQP was used. While second-order optimization methods (SQP) result in fast convergence, they are only viable in locally convex regions of the cost function. It is therefore useful to iterate initially using steepest descent, switching to SQP when the Hessian is determined to be positive definite.

B. Notation

The hybrid system model and notation used throughout this paper follow [17]. As in [17], slot derivative notation is used; i.e. $D_n f(arg_1, arg_2, ...)$ is the derivative of the function $f(\cdot)$ with respect to the argument at position n. $D_{arg}(...)$ is the derivative with respect to arg. The $\circ$ operator is used to represent linear mappings, for example $M \circ v = M \cdot v$, and $M \circ (v, u) = v^T [M] u$.

III. First Derivative of $J(\cdot)$

$DJ(\cdot)$ involves the derivatives of $J(\cdot)$ with respect to switching times and parameters. $DJ(\cdot)$ is the $N + M$ length vector

$$DJ(\cdot) = (D_{\tau_1} J, \ldots, D_{\tau_N} J, D_{p_1} J, \ldots, D_{p_M} J). \tag{5}$$

Derivations of $D_{\tau_i} J$ and $D_{p_i} J$ follow.

A. Calculating $D_{\tau_i} J(\cdot)$

Complete derivations of first-order partial derivatives of a cost function $J(\cdot)$ with respect to a switching time τ_i are derived in [1], [17]. Those results are presented here, as they are used directly in the second-order and parameter calculations.

Lemma 1: The first partial derivative of the cost function in Eq. (2) with respect to each switching time $\tau_i \ \forall \ i = 1, ..., N$ is calculated as

$$D_{\tau_i} J(\cdot) = \psi(\tau_i) \circ X^i, \tag{6}$$

where $\psi(t)$ is the n-length first-order adjoint found by solving the following backwards differential equation:

$$\dot{\psi}(t) = -D\ell(x(t)) - \psi(t) \circ D_1 f(x(t), t) \tag{7}$$
$$\psi(t_f) = 0.$$

$X^i \in \mathbb{R}^n$ is defined as shown below for compactness, following [17].

$$X^i = f_{i-1}(x(\tau_i), \tau_i) - f_i(x(\tau_i), \tau_i) \tag{8}$$

A proof of Lemma 1 can be found in [17].

B. Calculating $D_{p_i} J(\cdot)$

Lemma 2: The first partial derivative of the objective function with respect to a parameter p_i is calculated as

$$D_{p_i} J(\cdot) = \int_{t_0}^{t_f} \psi(t) \circ D_{p_i} f(x(t), t) dt, \tag{9}$$

where $\psi(t)$ is the same adjoint use in Lemma 1 calculated, using Eq. (7). Note that Eq. (9) is simply an inner product.

Proof: The derivation of Lemma 2 is similar to that of Lemma 1. The cost function from Eq. (2) is differentiated with respect to a parameter p_i, applying the chain rule as follows:

$$D_{p_i} J(\cdot) = \int_{t_0}^{t_f} D\ell(x(s)) \circ D_{p_i} x(s) ds.$$

This expression depends on the partial derivative of $x(t)$ with respect to a parameter p_i. $D_{p_i} x(s)$ is obtained by writing segments of the trajectory in integral form,

$$x(t_0) = x_0 \qquad x_k(t) = x_{k-1}(\tau_k) + \int_{\tau_k}^{t} f_k(x_k(s), s) ds,$$

and taking partial derivative of each segment $x_k(t)$ of the trajectory to obtain a linear differential equation for $D_{p_i} x_k(t)$.

$$\begin{aligned} D_{p_i} x_k(t) =& D_{p_i} x_{k-1}(\tau_k) + \int_{t_0}^{t} D_1 f_k(x(s), s) \circ D_{p_i} x_k(s) \\ &+ D_{p_i} f_k(x(s), s) ds \end{aligned}$$

Using the fundamental theorem of calculus, the above equation can be expressed in differential form:

$$\begin{aligned} D_{p_i} x_k(\tau_k) =& D_{p_i} x_{k-1}(\tau_k) \\ \frac{\partial}{\partial t} D_{p_i} x_k(t) =& D_1 f_k(x(t), t) \circ D_{p_i} x_k(t) + D_{p_i} f_k(x(t), t). \end{aligned}$$

The equation above is of the form $\dot{z}(t) = A(t)z(t) + B(t)$, which has the solution

$$\begin{aligned} D_{p_i} x_k(t) =& \Phi(t, \tau_k) D_{p_i} x_{k-1}(\tau_k) \\ &+ \int_{\tau_k}^{t} \Phi(t, \sigma) \circ D_{p_i} f_k(x(\sigma), \sigma) d\sigma, \end{aligned}$$

where the state transition matrix $\Phi(t, \tau_k)$ is the solution to $\dot{z}(t) = D_1 f_k(x(t), t) \circ z(t)$ [17]. For more information on the state transition matrix, see [18]. Because the initial condition $D_{p_i} x_{k-1}(\tau_k)$ depends recursively on the same expression for the previous segment of the trajectory and $D_{p_i} x(t_0) = 0$, $D_{p_i} x(t)$ can be expressed as a continuous trajectory as follows:

$$D_{p_i} x(t) = \int_{t_0}^{t} \Phi(t, \sigma) \circ D_{p_i} f(x(\sigma), \sigma) d\sigma. \tag{10}$$

Plugging the expression for $D_{p_i} x(t)$ from Eq. (10) into the expression for $D_{p_i} J$ yields

$$D_{p_i} J(\cdot) = \int_{t_0}^{t_f} D\ell(x(s)) \int_{t_0}^{s} \Phi(s, \sigma) \circ D_{p_i} f(x(\sigma), \sigma) d\sigma ds.$$

Switching the order of integration and pulling $D_{p_i} f(x(\sigma), \sigma)$ outside the inner integral, the following equation is obtained:

$$\begin{aligned} D_{p_i} J(\cdot) \quad = \quad & \int_{t_0}^{t_f} \left(\int_{\sigma}^{t_f} D\ell(x(s)) \circ \Phi(s, \sigma) ds \right) \\ & \circ D_{p_i} f(x(\sigma), \sigma) d\sigma. \end{aligned}$$

The operator $\psi(t)$ can thus be defined as the inner integral $\int_t^{t_f} D\ell(x(s)) \circ \Phi(s, t) ds$, which when differentiated with respect to t results in Eq. (7), the same backwards adjoint equation as used in the derivative with respect to a switching time. ■

The use of a backwards differential is advantageous when a trajectory is being analyzed over a finite time horizon. A single integration of $\psi(t)$ is used to calculate the values of the gradient with respect to switching times and with respect to all parameters, and can be calculated and stored once per iteration.

IV. Second Derivative of $J(\cdot)$

As mentioned, second-order derivative information provides sufficient conditions for optimality and can lead to much faster convergence rates. The Hessian with respect to switching times and parameters, $D_\tau^2 J(\cdot)$, is an $(N + M) \times (N + M)$ matrix, shown in block form in Eq. (3).

A. Calculating $D_\tau^2 J(\cdot)$

The second derivative of the cost function with respect to switching times is derived in [1], [17]. The notation once again follows that of [17] for compactness.

Theorem 1: The second derivative of the cost function with respect to two switching times τ_i and τ_j is calculated as follows:

$$\begin{aligned} D_{\tau_j} D_{\tau_i} J(\cdot) = & - D\ell(x(\tau_i)) \circ X^i \delta_i^j + \psi(\tau_i) \circ X^{i,j} + \\ & \Omega(\tau_i) \circ (\Phi(\tau_i, \tau_j) \circ X^j, X^i), \end{aligned} \tag{11}$$

where δ is the Kronecker delta. This equation involves the $n \times n$ second-order adjoint $\Omega(t)$, which is found by solving the following backwards differential equation:

$$\begin{aligned}\Omega(t_f) =& 0_{(n\times n)} \\ \dot{\Omega}(t) =& -D^2\ell(x(t)) - \psi(t) \circ D_1^2 f(x(t),t) - \\ & [D_1 f(x(t),t)]^T \circ \Omega(t) - \Omega(t) \circ D_1 f(x(t),t).\end{aligned} \tag{12}$$

The terms in $X^{i,j}$ are defined as

$$X^{i,j} = \begin{cases} D_1 f_i(x(\tau_i),\tau_i) \circ f_i(x(\tau_i),\tau_i) \\ +D_1 f_{i-1}(x(\tau_i),\tau_i) \circ f_{i-1}(x(\tau_i),\tau_i) \\ -2D_1 f_i(x(\tau_i),\tau_i) \circ f_{i-1}(x(\tau_i),\tau_i) \\ +D_2 f_{i-1}(x(\tau_i),\tau_i) - D_2 f_i(x(\tau_i),\tau_i) & i = j \\ \\ [D_1 f_{i-1}(x(\tau_i),\tau_j) - D_1 f_i(x(\tau_i),\tau_i)] \\ \circ \Phi(\tau_i,\tau j) \circ X^j & i > j. \end{cases} \tag{13}$$

A proof of Theorem 1 can be found in [17].

B. Calculating $D_p^2 J(\cdot)$

Theorem 2: The derivative of $J(\cdot)$ with respect to two parameters p_i and p_j can be calculated as follows:

$$\begin{aligned}D_{p_j} D_{p_i} J(\cdot) = & \int_{t_0}^{t_f} D_{p_i} f(x(t),t)^T \circ \Omega^{p_j}(t) \\ & + \psi(t) \circ [D_{p_j} D_{p_i} f(x(t),t) \\ & + D_1 D_{p_i} f(x(t),t) \circ D_{p_j} x(t)] dt,\end{aligned} \tag{14}$$

where $\Omega^{p_j}(t)$ is an n-length vector second-order adjoint equation, unique to each parameter, calculated by solving the differential equation below:

$$\begin{aligned}\Omega^{p_j}(t_f) =& 0_{(n)} \\ \dot{\Omega}^{p_j}(t) =& -D^2\ell(x(t),t) \circ D_{p_j} x(t) - \\ & [D_1 f(x(t),t)]^T \circ \Omega^{p_j}(t) - \\ & \psi(t) \circ [D_1^2 f(x(t),t) \circ D_{p_j} x(t) + \\ & D_{p_j} D_1 f(x(t),t)].\end{aligned} \tag{15}$$

Proof: Differentiating $D_{p_i} J(\cdot)$ with respect to the parameter p_j yields

$$\begin{aligned}D_{p_j} D_{p_i} J(\cdot) = & \int_{t_0}^{t_f} \frac{\partial}{\partial p_j} [\psi(t)] \circ D_{p_i} f(x(t),t) \\ & + \psi(t) \circ \frac{\partial}{\partial p_j} [D_{p_i} f(x(t),t)]\, dt\end{aligned}$$

A second-order adjoint, $\Omega^{p_j}(t) = \frac{\partial}{\partial p_j}[\psi(t)]$, is defined for the second derivative with respect to the parameters. $\Omega^{p_j}(t)$ is obtained by differentiating the expression for first-order adjoint, $\dot{\psi}(t)$, with respect to a parameter p_j (the initial condition remains zero), and integrating backwards in time as in the first-order derivation.

$\frac{\partial}{\partial p_j}[D_{p_i} f(x(t),t)]$ is calculated by differentiating $D_{p_i} f(x(t),t)$ with respect to a parameter p_j:

$$\begin{aligned}\frac{\partial}{\partial p_j} [D_{p_i} f(x(t),t)] = & \int_{t_0}^{t_f} D_{p_j} D_{p_i} f(x(s),s) \\ & + D_1 D_{p_i} f(x(s),s) \circ D_{p_j} x(s) ds.\end{aligned}$$

At this point, $\Omega^{p_j}(t)$ and $D_{p_j} D_{p_i} J(\cdot)$ can be substituted into the expression above to obtain Eq. (14). ■

C. Calculating $D_\tau D_p J(\cdot)$

In order to simultaneously optimize over switching times and parameters, the complete Hessian involves the derivative with respect to both a switching time and a parameter.

Theorem 3: The derivative of the cost function with respect to both a switching time τ_i and a parameter p_j is calculated as follows,

$$D_{\tau_i} D_{p_j} J(\cdot) = \psi(\tau_i) \circ X^{\tau,p} + [X^i]^T \circ \Omega^{p_j}(\tau_i) \tag{16}$$

where $\psi(\tau_i)$, X^i, $\Omega^{p_j}(\tau_i)$, are defined by Eqs. (7), (8), and (15), respectively. $X^{\tau,p}$ is defined as

$$\begin{aligned}X^{\tau,p} = & [D_1 f_{i-1}(x(\tau_i),\tau_i) - D_1 f_i(x(\tau_i),\tau_i)] \circ D_p x(\tau) \\ & + [D_p f_{i-1}(x(\tau_i),\tau_i) - D_p f_i(x(\tau_i),\tau_i)]\,.\end{aligned} \tag{17}$$

Proof: Differentiating $D_{\tau_i} J(\cdot)$ in Eq. (6) with respect to the parameter p_j yields

$$D_{p_j} D_{\tau_i} J(\cdot) = \psi(\tau_i) \circ X^{\tau,p} + \frac{\partial}{\partial p_j} \psi(\tau_i) \circ X^i.$$

$X^{\tau,p}$ represents $\frac{\partial}{\partial p_j} X^i$, the derivative of the initial conditions X^i with respect to a parameter. Equation (17) is obtained by differentiating and applying the chain rule to Eq. (8).

The second term involves $\frac{\partial}{\partial p_j}\psi(\tau_i)$, which is the same second-order adjoint $\Omega^{p_j}(t)$ derived previously, evaluated at the switching time τ_i. ■

The adjoint equations (7) and (15), derived in the context of hybrid systems, are derived in [2] for continuous systems using multiplier methods. The derivation of the second order derivative with respect to parameters presented in this paper, in addition to applying to hybrid scenarios, is generalized to the cross-derivative terms between switching times and parameters, which is shown to be critical for fast convergence.

V. Example: The Skid-Steered Vehicle

In the following sections, the proposed estimation algorithms are applied to the skid-steered vehicle, for both

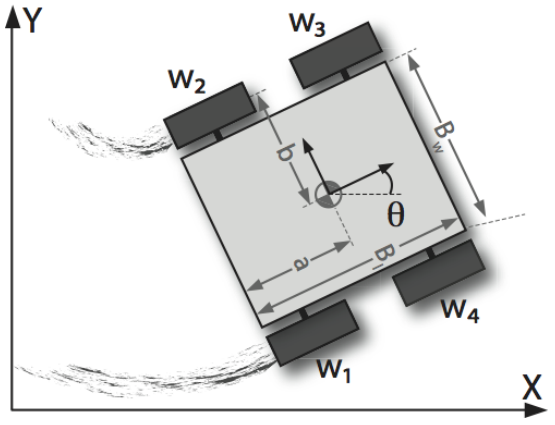

Fig. 2. Skid-Steered vehicle model used in simulation

simulated and experimental data. A diagram of the SSV model used is shown in Fig. 2. The vehicle is made up of four wheels connected to a rigid body. The vehicle turns if the applied differential torque is large enough to cause slipping between the tires and the ground, resulting in skidding. The coefficient of friction for the SSV example is treated as an unknown parameter. The wheel-ground interaction is modeled as viscous friction.

The vehicle configuration is $x = (X, \dot{X}, Y, \dot{Y}, \theta, \dot{\theta})$,where X and Y are Cartesian coordinates with respect to the vehicle center of mass, and θ represents the heading of the vehicle in the global frame. Only the modes in which all wheels are slipping (turning) or all wheels are sticking (driving straight) are considered. The equations of motion are adopted from [1] and are shown below for a vehicle that turns once, switching from sticking to slipping, and back to sticking.

$$\text{In stick mode: } \begin{cases} \ddot{X} = \frac{(F_1+F_2)\cos\theta(t) - c_1\dot{X}(t)}{(4m_w+m_b)} \\ \ddot{Y} = \frac{(F_1+F_2)\sin\theta(t) - c_1\dot{Y}(t)}{(4m_w+m_b)} \\ \ddot{\theta} = 0 \end{cases}$$

$$\text{In slip mode: } \begin{cases} \ddot{X} = \frac{(F_1+F_2)\cos\theta(t) - c_2\dot{X}(t)}{(4m_w+m_b)} + \\ g\mu_k \sin\theta(t)\left(-\sin\theta(t)\dot{X}(t) + \cos\theta(t)\dot{Y}(t)\right) \\ \ddot{Y} = \frac{(F_1+F_2)\sin\theta(t) - c_2\dot{Y}(t)}{(4m_w+m_b)} - \\ g\mu_k \cos\theta(t)\left(-\sin\theta(t)\dot{X}(t) + \cos\theta(t)\dot{Y}(t)\right) \\ \ddot{\theta} = \frac{12b(F_1-F_2) - 12a^2 g\mu_k(4m_w+m_b)\dot{\theta}(t)}{4m_w(12a^2+12b^2)+m_b(B_l^2+B_w^2)} \end{cases}$$

$$\dot{x}(t) = f(x(t),t) = \begin{cases} \text{sticking} & 0 \le t < \tau_1 \\ \text{slipping} & \tau_1 \le t < \tau_2 \\ \text{sticking} & \tau_1 \le t < 1 \end{cases}$$

In these equations F_1 and F_2 are the transformed wheel torques sent to the wheel pairs on each side of the vehicle, μ_k is the coefficient of friction, g is the gravitational constant, and m_w and m_b are the masses of the wheel and car body, respectively. B_l and B_w are the length and width of the vehicle body, a and b are the distances from the wheels to the center of mass in each dimension. The incremental cost function used in the simulations and experiments was $\ell(x(t),t) = \frac{1}{2}\left(x(t) - x_{ref}(t)\right)^T \left(x(t) - x_{ref}(t)\right)$.

A. Simulation

The system was simulated using Mathematica. The equations of motion were used to simulate measured data, which was sampled at one second intervals, interpolated and low-pass filtered to simulate coarsely sampled GPS measurements. Interpolation is necessary as the algorithm assumes continuous state variables, and filtering accounts for some process noise and improves robustness. The reference trajectory was generated using $\mu_k = 0.8$, $\tau_1 = 5$, $\tau_2 = 10.5$. The estimation algorithm was initialized to $\mu = 0.77$, $\tau_1 = 4.7$, $\tau_2 = 9.7$.

Figure 3 shows logarithmic plots of the norm of the gradient at each iteration using three different optimization techniques to obtain the transition-time and parameter estimates from simulated data: steepest descent using only first-order derivative information, SQP using a block-diagonal Hessian and SQP using the complete Hessian in simulation. Using steepest descent, the algorithm converged to the correct values after about 700 iterations. Using SQP with the full Hessian, the correct values were determined after only 7 iterations. When SQP was performed using a block diagonal approximation of the Hessian, the convergence does not exhibit the fast quadratic performance of the full Hessian including the cross-derivative terms.

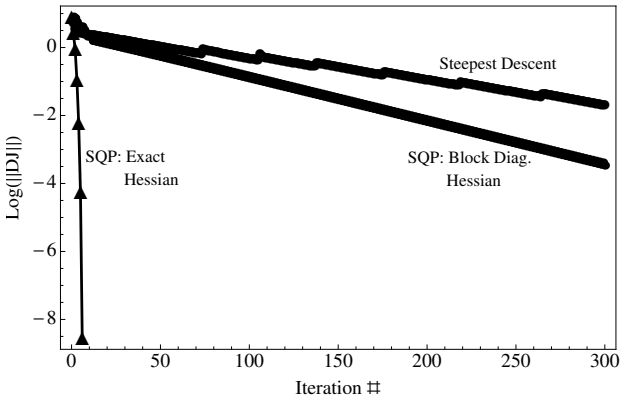

Fig. 3. The logarithm of the norm of the gradient of the cost function, shown at every iteration for first-order and approximate and exact second-order methods.

B. Experiment

The vehicle shown in Fig. 1 was used to demonstrate the estimation technique developed in an experimental system. The vehicle position was recorded using an on-board GPS, sampled at 1 Hz.

Figure 4 shows a representative plot of the raw GPS data collected during the experiment, as well as the interpolated and filtered curve used as the reference trajectory x_{ref} in the optimization algorithm (dashed gray line). The trajectory

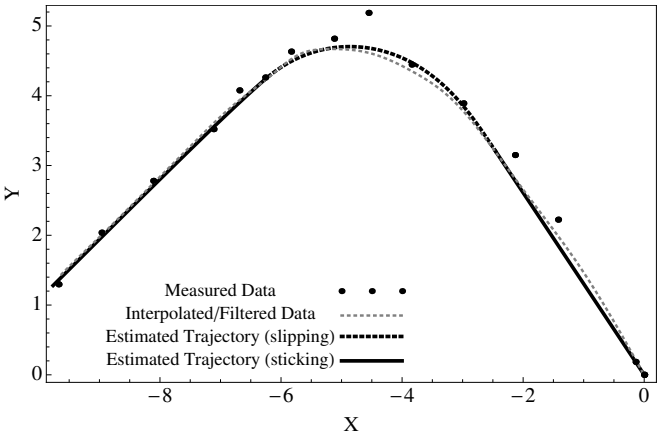

Fig. 4. Plot of the measured position data as well as the interpolated and filtered curve used as a reference for the estimation. The simulated trajectory generated using the values that the algorithm converged to is shown in black.

that corresponds to the optimal estimate of the values of the switching times and parameters is plotted in black, and follows the smoothed interpolation almost exactly. The algorithm converges to $\mu = 0.85$, $\tau_1 = 4.93$, $\tau_2 = 10.52$ in six iterations, starting from initial values of $\mu = 0.75$, $\tau_1 = 5$, $\tau_2 = 11$. Although the algorithm is initialized to values that are relatively close to the correct values, choosing initial conditions further away would still result in the same estimate, but would require initial iteration using steepest descent before reaching a locally convex region second-order methods are viable.

The torques, sent to the vehicle as PWM signals, were programmed to transition at 5 and 10 seconds. Battery discharge, lag due to the motors and transitioning from stick to slip likely resulted in variation in actual transition times. Values for the coefficient of friction of rubber on asphalt range from 0.6-0.85 [19]. The estimate calculated using the derived algorithm is within this range. The generated trajectory fits the interpolation of the data quite well, and improvements to the experimental system as well as data filtering would likely provide even better results.

VI. Conclusion

An algorithm for estimating both mode transition times and parameters using first- and second-order optimization methods for a hybrid system operating in uncertain conditions is presented. The main contributions are analytical derivations of the Hessian and gradient with respect to mode transition times and parameters. The results are proven concisely, relying on standard calculus techniques that generalize to hybrid systems and cross-derivative terms between the switching times and parameters. Simulation results demonstrate dramatic increase in convergence rates using second-order methods within the SQP framework using the exact Hessian. Fast convergence is critical for real-time applications. Simulations and experimental results demonstrate the ability of the algorithm to perform well given coarsely sampled experimental data.

Future work will involve formally characterizing the robustness with respect to measurement noise and initial conditions, and extending the method to optimize for mode order as well as transition time. Experimentation in different environmental conditions and vehicle maneuvers is also planned.

Acknowledgment

This material is based upon work partially supported by the National Science Foundation under Grant IIS-0917837. Any opinions, findings, and conclusions or recommendations expressed in this material are those of the author(s) and do not necessarily reflect the views of the National Science Foundation.

References

[1] T. Caldwell and T. Murphey, "Switching mode generation and optimal estimation with application to skid-steering," *Automatica*, vol. 47, no. 1, pp. 50 – 64, 2011.

[2] D. Ozyurt, B. Derya, and P. Barton, "Cheap second order directional derivatives of stiff ode embedded functionals," *SIAM Journal of Scientific Computing*, vol. 26, no. 5, pp. 1725–1743, May 2005.

[3] G. Anousaki and K. Kyriakopoulos, "A dead-reckoning scheme for skid-steered vehicles in outdoor environments," in *IEEE Int. Conf. on Robotics and Automation (ICRA)*, vol. 1, April 2004, pp. 580 – 585.

[4] L. Ojeda, D. Cruz, G. Reina, and J. Borenstein, "Current-based slippage detection and odometry correction for mobile robots and planetary rovers," *IEEE Transactions on Robotics*, vol. 22, no. 2, pp. 366 –378, April 2006.

[5] R. Balakrishna and A. Ghosal, "Modeling of slip for wheeled mobile robots," *IEEE Transactions on Robotics and Automation*, vol. 11, no. 1, pp. 126 –132, Feb 1995.

[6] E. Velenis, P. Tsiotras, and J. Lu, "Aggressive maneuvers on loose surfaces: Data analysis and input parametrization," in *MED Conf. on Control Automation*, June 2007, pp. 1–6.

[7] C. Canudas-de-Wit, P. Tsiotras, E. Velenis, M. Basset, and G. Gissinger, "Dynamic friction models for road/tire longitudinal interaction," pp. 189–226, 2003.

[8] J. Yi, D. Song, J. Zhang, and Z. Goodwin, "Adaptive trajectory tracking control of skid-steered mobile robots," in *IEEE Int. Conf. on Robotics and Automation (ICRA)*, April 2007, pp. 2605 –2610.

[9] K. Iagnemma, K. Shinwoo, H. Shibly, and S. Dubowsky, "Online terrain parameter estimation for wheeled mobile robots with application to planetary rovers," *IEEE Transactions on Robotics*, vol. 20, no. 5, pp. 921 – 927, Oct. 2004.

[10] L. Ray, "Estimation of terrain forces and parameters for rigid-wheeled vehicles," *IEEE Transactions on Robotics*, vol. 25, pp. 717–726, June 2009.

[11] S. Zibin, Y. Zweiri, L. Seneviratne, and K. Althoefer, "Non-linear observer for slip estimation of skid-steering vehicles," in *IEEE Int. Conf. on Robotics and Automation (ICRA)*, May 2006, pp. 1499 – 1504.

[12] L. Caracciolo, A. de Luca, and S. Iannitti, "Trajectory tracking control of a four-wheel differentially driven mobile robot," in *IEEE Int. Conf. on Robotics and Automation (ICRA)*, vol. 4, 1999, pp. 2632 –2638.

[13] E. Velenis, P. Tsiotras, C. Canudas-de-Wit, and M. Sorine, "Dynamic tire friction models for combined longitudinal and lateral vehicle motion," *Vehicle System Dynamics*, vol. 43, no. 1, pp. 3–29, 2005.

[14] T.J.Debus, P. Dupont, and R. Howe, "Contact state estimation using multiple model estimation and hidden markov models," *International Journal of Robotics Research*, vol. 23, no. 4-5, pp. 399–413, 2004.

[15] A. Damle and L. Pao, "Simultaneous numerical optimization for data association and parameter estimation," in *IEEE Int. Conf. on Decision and Control (CDC)*, 2011.

[16] J. Nocedal and S. Wright, *Numerical Optimization*. Springer, 2006.

[17] E. Johnson and T. Murphey, "Second-order switching time optimization for nonlinear time-varying dynamic systems," *IEEE Transactions on Automatic Control*, vol. 56, no. 8, pp. 1953 –1957, Aug. 2011.

[18] J. P. Hespanha, *Linear Systems Theory*. Princeton, New Jersey: Princeton Press, Sep. 2009.

[19] J. Stephens, *Kempe's Engineers Year Book*, ser. Kempe's Engineer's Year Book Series. CMP Information, 2001.